Occasional Note Met O 21 75/3

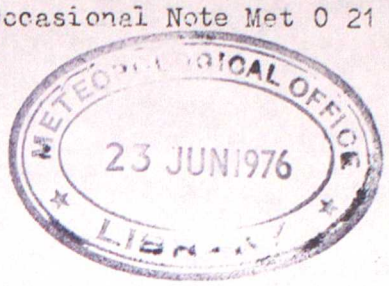

122230

NUMERICAL INTEGRATION OF FLOW IN A ROTATING ANNULUS

I: AXISYMMETRIC MODEL

L Farnell

and

R A Plumb

Geophysical Fluid Dynamics Laboratory

Meteorological Office

Bracknell, Berkshire

December 1975

Contents

	Definition of symbols	(ii)
1	Introduction	1
2	Equations governing the system	3
	2.1 The governing equations	3
	2.2 Integrals of the governing equations	5
3	The stretched grid	10
	3.1 Determination of the grid	10
	3.2 Theory of finite differences on a stretched grid	14
4	The finite difference equations	17
	4.1 Formulation of the nonlinear advection terms	17
	4.2 Representation of the diffusion terms	19
	4.3 Finite difference form of the governing equations	20
	4.4 Integrals of the finite difference equations	23
	4.5 The Poisson equation	31
5	Method of solution	34
	5.1 ADI method for the Poisson equation	34
	5.2 General outline of procedure	38
6	Summary	39
	References	40

Definition of symbols

a	inner radius of annulus
A	(total angular momentum)/$2\pi\rho_0$
$\mathcal{A}$	advection operator
b	outer radius of annulus
c	specific heat of fluid
c_r, c_z	maximum flow or wave speeds in radial and vertical directions
C_{PK}	energy conversion rate
d	depth of annulus
$\mathcal{D}$	diffusion operators
E	Ekman number
E_K	(total kinetic energy)/$2\pi\rho_0$
E_P	(total potential energy)/$2\pi\rho_0$
$\mathcal{F}$	flux terms
g	acceleration due to gravity
i	radial grid index
I	number of principal grid points in radial direction
k	vertical grid index
K	number of principal grid points in vertical direction
m	time index
$\mathcal{M}$	mass flux contribution to angular momentum balance
Q	(total heat content)/$2\pi c\rho_0$
r	radial co-ordinate
r_i	co-ordinate of principal radial grid points
$\tilde{r}_i$	co-ordinate of secondary radial grid points
t	time
T	temperature
$T_{i,k}^m$	temperature at $r = \tilde{r}_i$, $z = \tilde{z}_k$, $t = m.\Delta t$
T_0	reference temperature
(u,v,w)	velocity components in (r,θ,z)
$u_{i,k}^m$	radial velocity at $r = r_i$, $z = \tilde{z}_k$, $t = m.\Delta t$
$v_{i,k}^m$	azimuthal velocity at $r = \tilde{r}_i$, $z = \tilde{z}_k$, $t = m.\Delta t$
$w_{i,k}^m$	vertical velocity at $r = \tilde{r}_i$, $z = z_k$, $t = m.\Delta t$
(x,y)	stretched co-ordinates
z	vertical co-ordinate
α	volume coefficient of expansion
δ	finite difference derivative
$\delta_1, \delta_2, \delta_3$	boundary layer thicknesses
$\delta r_i, \tilde{\delta r}_i$	radial grid increments
$\delta z_k, \tilde{\delta z}_k$	vertical grid increments

Δ	divergence
Δt	timestep
Δx	radial grid increment in stretched co-ordinate
Δy	vertical grid increment in stretched co-ordinate
θ	azimuthal co-ordinate
κ	coefficient of thermal diffusion
ν	coefficient of kinematic viscosity
π	pressure $/ \rho_0$
ρ	density perturbation
ρ_0	mean density
ρ_1, ρ_2	expansion coefficients
σ	buoyancy
τ_i	iteration parameters

1 INTRODUCTION

This report describes the formulation of a numerical model to integrate the Navier-Stokes equations for a viscous, thermally conducting liquid contained in a rotating annulus, ie the system is bounded (in (r, θ, z) cylindrical co-ordinates with the axis of rotation at $r = 0$) at $r = a, b$ $(b > a)$ and $z = 0, d$. The model described here integrates the equations for axisymmetric motions (ie $\partial/\partial\theta = 0$); a three-dimensional model will be described in a subsequent report.

The program is specifically written in such a way as to allow the model to be used with a variety of boundary conditions. These conditions may be fixed temperature or heat flux, rigid or "slippery" (ie stress-free), even source-sink arrangements may be applied (though this latter case introduces some small error terms into the finite-difference integrals of the motion; at the time of writing. the significance of these terms has not been tested). In order to allow detailed comparison of the numerical results with those of corresponding laboratory experiments, coefficients of viscosity, thermal conductivity and expansion are allowed to vary (in a specified manner) with temperature.

Computer simulations of thermal convection in a rotating annulus have been produced by a number of workers, notably Williams (1967, 1969) and the present model is similar to that of Williams (1967) in many respects. The major differences are as follows.

(i) Non-uniform grid.

Exchange of heat and momentum between fluid and boundaries takes place in boundary layers on the sidewalls and endwalls. The nature and thickness of these boundary layers depends on the boundary conditions of the problem; a rotating fluid has Ekman boundary layers on the endwalls of thickness

$$\delta_1 \simeq d\,\varepsilon^{1/2} \qquad (1.1)$$

where $E = \nu/\Omega d^2$ is the Ekman number. The mass flux through these layers is accommodated in sidewall boundary layers, whose thickness is

$$\delta_2 \simeq (b-a)\, E^{1/3} \tag{1.2}$$

(Greenspan, 1968). Additionally, in problems of thermal convection in a differentially heated rotating annulus, thermal boundary layers are formed on the sidewalls. Their thickness varies with distance along the sidewall, but is of magnitude

$$\delta_3 \sim d \left(\frac{\kappa \nu}{\alpha g \Delta T\, d^3} \right)^{1/4}. \tag{1.3}$$

In laboratory experiments, these layers are usually thin compared to the dimensions of the apparatus. If such flows were modelled using a regular finite-difference mesh, a large number of points would be required in order to resolve these layers, but much of the resolution so obtained, in the interior of the fluid, would be unnecessary. Consequently, in order that flows in the parameter range appropriate to laboratory experiments may be simulated without making unrealistic demands in terms of computing time and storage, the grids are stretched in such a way as to resolve fine scales near the boundaries without the need for a large number of points in the interior. The means by which this is achieved is outlined in § 3.1.

(ii) Diffusion terms

Because of the small grid size required in the boundary layers, the timestep condition necessary to ensure stability of the diffusion terms in a "leap-frog" time-differencing scheme becomes very restrictive. This problem is avoided

through use of the DuFort-Frankel scheme to respresent the diffusion terms; its use is described in § 4.2.

(iii) Angular momentum advection.

The nonlinear terms in the zonal equation of motion are formulated in such a way that the angular momentum integral contains no spurious terms (other than those small error terms that vanish as $\Delta t \to 0$).

(iv) Solution of the Poisson equation.

The continuity equation is satisfied at all times by satisfying a Poisson equation for pressure at each timestep. This is achieved by an iterative technique, rather than the more efficient Fourier transform method, which is not well suited to non-uniform grids.

The continuous equations and their integrals are presented in Section 2. In Section 3, the method by which the grids are determined is described, together with a discussion of finite differences on a stretched mesh. The finite-difference equations are given in Section 4, and the finite-difference form of the physically important integrals are derived. An outline of the method by which the solution is evaluated is given in Section 5.

2 EQUATIONS GOVERNING THE SYSTEM

2.1 The Governing Equations

The Boussinesq equations for axisymmetric flow of a rotating fluid are, in cylindrical polar co-ordinates, as follows:

(i) the equations of motion

$$\frac{\partial u}{\partial t} + u\frac{\partial u}{\partial r} + w\frac{\partial u}{\partial z} = -\frac{\partial \Pi}{\partial r} + v\left(2\Omega + \frac{v}{r}\right) \cdots \quad (2.1)$$

$$\cdots + \Delta^2(v,u) + \frac{1}{r}\frac{\partial}{\partial r}(ru)\frac{\partial v}{\partial r} + \frac{\partial w}{\partial r}\frac{\partial v}{\partial z},$$

$$\frac{\partial v}{\partial t} + u\frac{\partial v}{\partial r} + w\frac{\partial v}{\partial z} = -u\left(\frac{v}{r}+2\Omega\right) + \Delta^2(\nu, v) \,,$$

(2.2)

$$\frac{\partial w}{\partial t} + u\frac{\partial w}{\partial r} + w\frac{\partial w}{\partial z} = -\frac{\partial \pi}{\partial z} - \frac{g\epsilon}{\epsilon_0} + \tilde{\Delta}^2(\nu, w) \ldots$$

$$\ldots + \frac{\partial u}{\partial z}\frac{\partial \epsilon}{\partial r} + \frac{\partial w}{\partial z}\frac{\partial \epsilon}{\partial z} \,; \qquad (2.3)$$

(ii) the continuity equation

$$\frac{1}{r}\frac{\partial}{\partial r}(ru) + \frac{\partial w}{\partial z} = 0 \,, \qquad (2.4)$$

and (iii) the heat equation

$$\frac{\partial T}{\partial t} + u\frac{\partial T}{\partial r} + w\frac{\partial T}{\partial z} = \tilde{\Delta}^2(\kappa, T) \,, \qquad (2.5)$$

where the diffusion operators are

$$\Delta^2(\lambda, A) = \frac{1}{r^2}\frac{\partial}{\partial r}\left\{\lambda r^3 \frac{\partial}{\partial r}\left(\frac{A}{r}\right)\right\} + \frac{\partial}{\partial z}\left(\lambda\frac{\partial A}{\partial z}\right),$$

and (2.6)

$$\tilde{\Delta}^2(\lambda, A) = \frac{1}{r}\frac{\partial}{\partial r}\left(\lambda r\frac{\partial A}{\partial r}\right) + \frac{\partial}{\partial z}\left(\lambda\frac{\partial A}{\partial z}\right).$$

The system of equations (2.1) - (2.5) is closed by an equation of state, which we take to be of the form

$$\frac{\rho}{\rho_0} = \rho_1 (T - T_0) + \rho_2 (T - T_0)^2 , \tag{2.7}$$

where T_0 is some standard reference temperature.

2.2 Integrals of the governing equations

(a) Angular Momentum Balance.

The total angular momentum of the fluid is $2\pi\rho_0 A$, where

$$A = \int_a^b \int_0^d v\, r^2 \, dr \, dz . \tag{2.8}$$

Integration of equation (2.2) yields an equation for the evolution of angular momentum, which we write in the form

$$\frac{dA}{dt} = \mathcal{F}_A^{(D)} + \mathcal{F}_A^{(R)} + \mathcal{F}_A^{(V)} . \tag{2.9}$$

In this equation, $\mathcal{F}_A^{(D)}$ is the dynamical flux of relative angular momentum through the boundaries:

$$\mathcal{F}_A^{(D)} = -\int_a^b \left[wv \right]_{z=0}^{z=d} r^2 \, dr - \int_0^d \left[r^2 uv \right]_{r=a}^{r=b} dz . \tag{2.10}$$

The second term is the contribution due to advection of the rotational angular momentum of the annulus; it may be written

$$\mathcal{J}_A^{(R)} = -2\Omega \int_a^b \mathcal{M}(r).r.dr \quad , \tag{2.11}$$

where $\mathcal{M}(\xi)$ is the mass flux across a surface $r = \xi$, so that

$$\mathcal{M}(r) = \int_0^d ru.dz \quad . \tag{2.12}$$

In particular, if the upper and lower boundaries are rigid, so that $w(r,0) = 0$, $w(r,d) = 0$, then $\mathcal{M}$ is constant and we find

$$\mathcal{J}_A^{(R)} = -\Omega(b^2-a^2)\mathcal{M} \tag{2.13}$$

where

$$\mathcal{M} = a\int_0^d u(a,z)\,dz = b\int_0^d u(b,z).dz \quad . \tag{2.14}$$

Finally, $\mathcal{J}_A^{(v)}$ is the viscous flux of angular momentum into the system,

$$\mathcal{J}_A^{(v)} = \int_0^d \left[\nu r^3 \frac{\partial}{\partial r}\left(\frac{v}{r}\right)\right]_{r=a}^{r=b}.dz + \int_a^b \left[\nu \frac{dv}{dz}\right]_{z=0}^{z=d}.r^2\,dr \quad . \tag{2.15}$$

(b) Heat Balance.

The heat content of the fluid is $2\pi\rho_0 c\, Q$, where

$$Q = \int_a^b \int_0^d T \cdot r \, dr \, dz \quad . \tag{2.16}$$

Equation (2.5) integrates to give

$$\frac{dQ}{dt} = \mathcal{F}_Q^{(D)} + \mathcal{F}_Q^{(V)} \quad , \tag{2.17}$$

where the dynamical heat flux is

$$\mathcal{F}_Q^{(D)} = -\int_0^d \left[r u T \right]_{r=a}^{r=b} dz - \int_a^b \left[w T \right]_{z=0}^{z=d} r \, dr \quad , \tag{2.18}$$

and $\mathcal{F}_Q^{(V)}$ is the diffusive flux of heat from the boundaries:

$$\mathcal{F}_Q^{(V)} = \int_0^d \left[\kappa r \frac{dT}{dr} \right]_{r=a}^{r=b} dz + \int_a^b \left[\kappa \frac{dT}{dz} \right]_{z=0}^{z=d} r \, dr \quad . \tag{2.19}$$

(c) Kinetic Energy.

The total kinetic energy is $2\pi\rho_0 \mathcal{E}_K$, with

$$\mathcal{E}_K = \frac{1}{2} \int_0^d \int_a^b (u^2 + v^2 + w^2) \cdot r \, dr \, dz \quad ; \tag{2.20}$$

integration of the equations of motion (2.1) - (2.3) gives

$$\frac{dE_K}{dt} = C_{PK} + \mathcal{F}_K^{(D)} - D_K \,. \tag{2.21}$$

The first term on the right hand side of (2.21) is the rate of conversion of potential to kinetic energy,

$$C_{PK} = -\int_0^d\int_a^b g w \frac{\varrho}{\varrho_0} \, r \, dr \, dz \tag{2.22}$$

The flux of kinetic and internal energy into the fluid at the boundaries is

$$\mathcal{F}_K^{(D)} = -\int_0^d \left[ru \left\{ \Pi + \tfrac{1}{2}(u^2+v^2+w^2) \right\} \right]_{r=a}^{r=b} dz \; \ldots$$

$$\ldots - \int_a^b \left[w \left\{ \Pi + \tfrac{1}{2}(u^2+v^2+w^2) \right\} \right]_{z=0}^{z=d} r \, dr \,, \tag{2.23}$$

while

$$D_K = -\int_a^b\int_0^d \left\{ u \left[\Delta^2(r,u) + \frac{1}{r}\frac{\partial}{\partial r}(ru)\frac{\partial \varrho}{\partial r} + \frac{\partial w}{\partial r}\frac{\partial \varrho}{\partial z} \right] \right.$$

$$\left. \ldots + v\,\Delta^2(r,v) + w \left[\tilde{\Delta}^2(r,w) + \frac{\partial u}{\partial z}\frac{\partial \varrho}{\partial r} + \frac{\partial w}{\partial z}\frac{\partial \varrho}{\partial z} \right] \right\} r \, dr \, dz \tag{2.24}$$

is the rate of dissipation of kinetic energy.

(d) Potential Energy.

Defining

$$\mathcal{E}_p = \int_a^b \int_0^d g \frac{\epsilon}{\rho_0} r z \, dr \, dz \,, \tag{2.25}$$

so that $2\pi\rho_0 \mathcal{E}_p$ is the total potential energy of the system, we have

$$\frac{d\mathcal{E}_p}{dt} = \frac{g}{\rho_0} \int_a^b \int_0^d \frac{\partial \rho}{\partial t} r \, dr \, z \, dz \,. \tag{2.26}$$

Substituting from the equation of state (2.7) and the heat equation (2.5), this may be written

$$\frac{d\mathcal{E}_p}{dt} = -C_{pK} + \mathcal{F}_p^{(D)} - D_p \,, \tag{2.27}$$

where the energy conversion term C_{pK} is defined by equation (2.22). The flux of potential energy through the boundaries is

$$\mathcal{F}_p^{(D)} = -\frac{g}{\rho_0} \int_0^d \left[r u \rho \right]_{r=a}^{r=b} z \, dz - \frac{g}{\rho_0} \int_a^b \left[w \rho z \right]_{z=0}^{z=d} r \, dr \,, \tag{2.28}$$

and the rate of dissipation of potential energy is given by

$$D_r = -g \int_0^d \int_a^b \{\rho_1 + 2\rho_2 (T-T_0)\} \tilde{\Delta}^2(\kappa, T)\, r\,dr\,z\,dz \,. \qquad (2.29)$$

3 THE STRETCHED GRID

3.1 Determination of the grid

In order to provide increased resolution in the region of the sidewall and endwall boundary layers, the grid is stretched by mapping the radial and vertical co-ordinates (r, z) into new co-ordinates (x, y), choosing suitable mapping functions. A regular grid is then defined in (x, y) space. Averaging is reduced (and hence accuracy improved) by staggering the grid points in the same way as in the model of Williams (1969); the grid is shown in Figure 1. The last row of radial velocity (u) points and last column of vertical velocity (w) points are not used, nor are some of the corner points.

The mapping function used, in both radial and vertical directions, is a hyperbolic tangent, so that we write

$$r - \tfrac{1}{2}(b+a) = \xi(x) = r_0 \tanh(\alpha_r x)$$

$$\text{and } z - \tfrac{1}{2}d = \eta(y) = z_0 \tanh(\alpha_z y) \qquad (3.1)$$

where the ranges of the co-ordinates are fixed so that, eg, in the radial direction

$$-x_1 = x_{I-1} = \tfrac{1}{2}(b-a) \qquad (3.2)$$

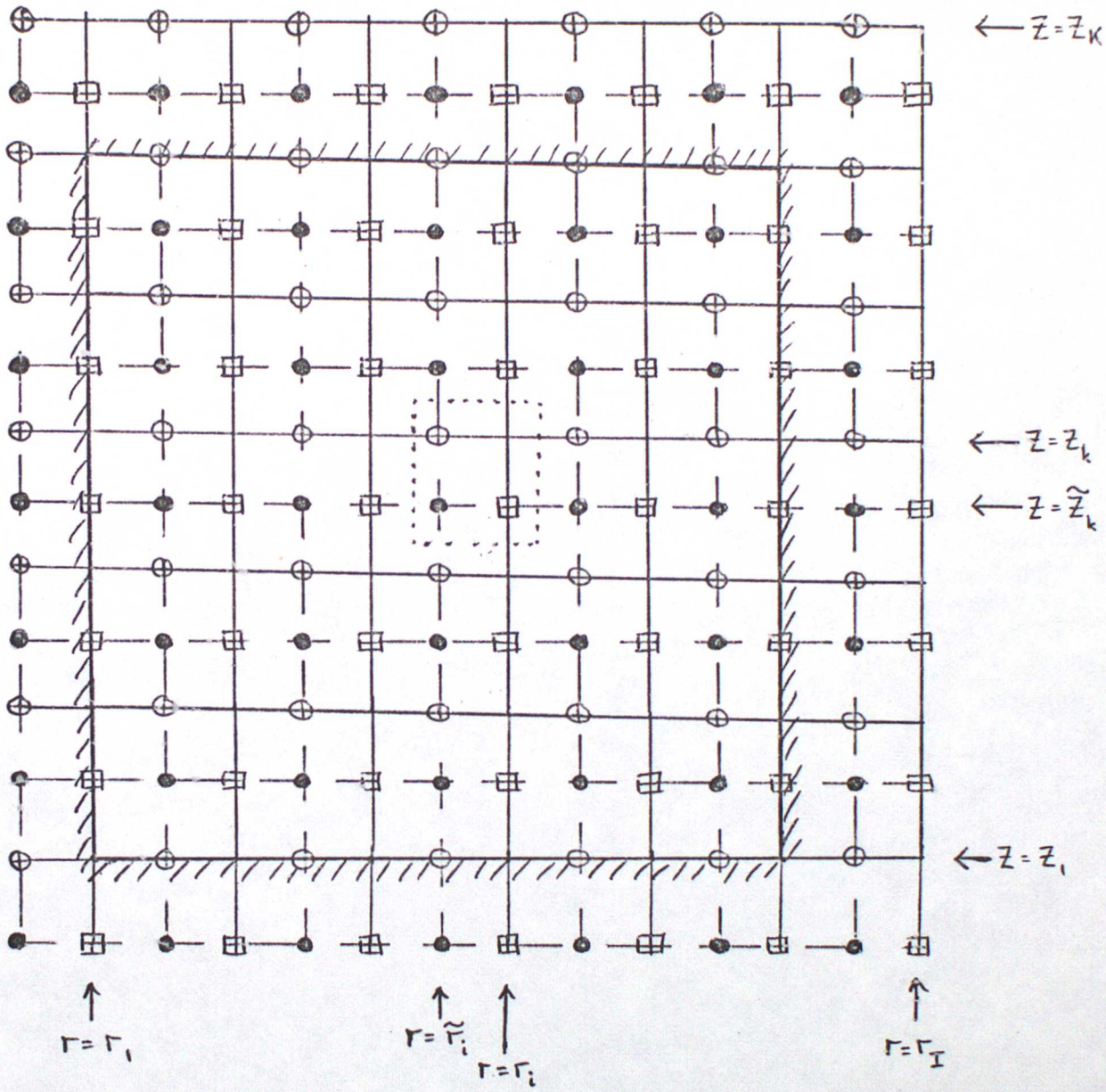

Figure 1

The finite-difference grid (mapped in the regular (x, y) space). The location of the boundaries is marked by shading; the (i, k) cell is delineated by the dotted line. Flow variables are evaluated at the following points:

- $\oplus$ - vertical velocity w
- $\boxplus$ - radial velocity u
- $\bullet$ - temperature T, azimuthal velocity v, pressure Π.

The form of the stretching function $\xi(x)$ is shown in Figure 2 ($\eta(y)$ is, of course, of similar form).

To ensure that $r_1 = a$ we require, from equations (3.1) and (3.2), that

$$\frac{b-a}{2r_0} = \tanh\left[\frac{\alpha_r}{2}(b-a)\right]. \tag{3.3}$$

The degree of stretching is determined by selecting a nominal first grid increment Δr , and then demanding that the gradient of the function on the boundary be

$$\frac{d\xi}{dx} = \frac{\Delta r}{\Delta x} = g , \tag{3.4}$$

where Δx is the grid increment in x-space; from (3.2), it is

$$\Delta x = \frac{(b-a)}{(I-2)} . \tag{3.5}$$

Hence, differentiating the first of equations (3.1), and using (3.3), we find

$$g = \alpha_r r_0 \left\{1 - \left(\frac{b-a}{2r_0}\right)^2\right\} . \tag{3.6}$$

Eliminating α_r between equations (3.3) and (3.6), we find r_0 from the relation

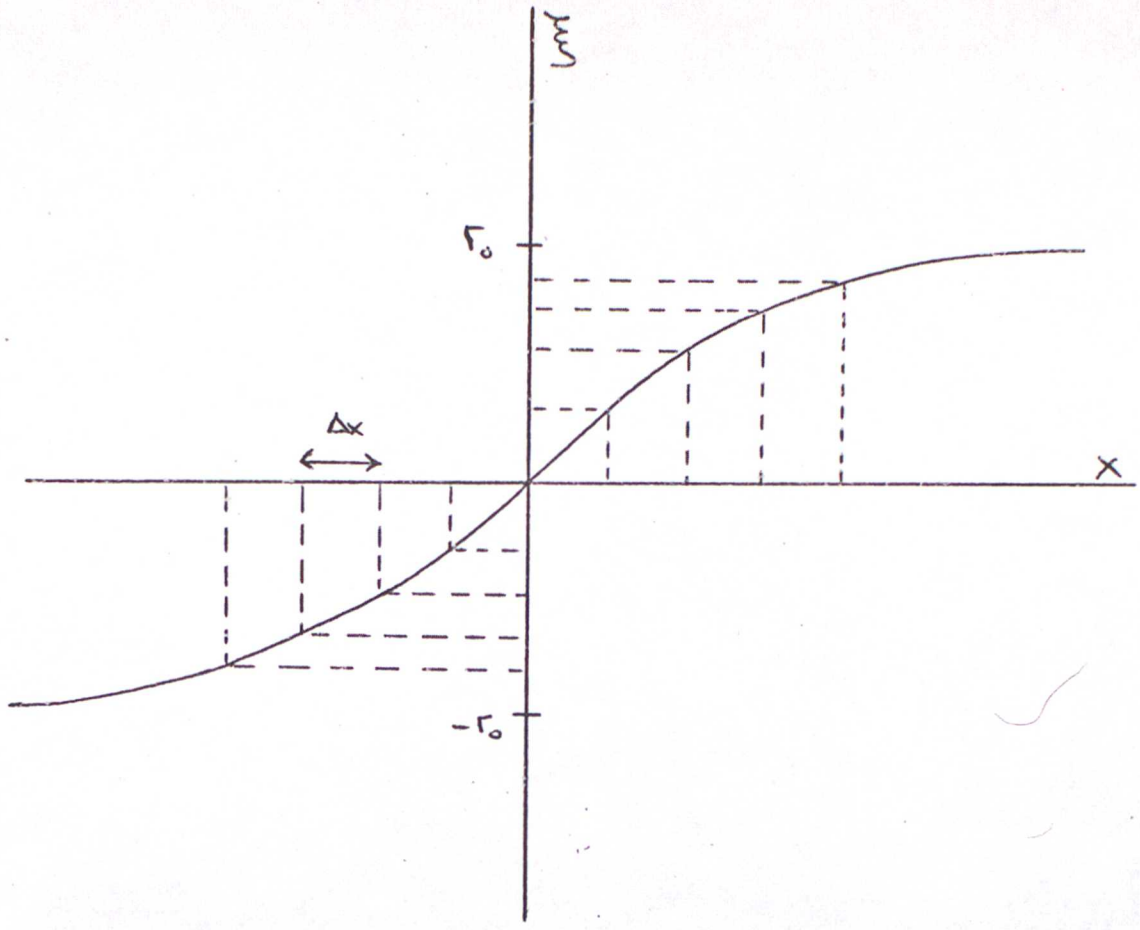

Figure 2

The mapping function $\xi(x) = r_0 \tanh(\alpha_r x)$. The regular grid (on the x-axis) and corresponding stretched grid (on the ξ-axis) are schematically depicted.

$$\Gamma_0 = \frac{b-a}{2\gamma_0} \tag{3.7}$$

where γ_0 is the positive solution of the equation

$$\gamma_0 = \tanh\left\{\zeta \cdot \frac{\gamma_0}{1-\gamma_0^2}\right\}. \tag{3.8}$$

The function

$$\Im(\gamma) = \tanh\left\{\zeta \frac{\gamma}{1-\gamma^2}\right\} - \gamma \tag{3.9}$$

is shown in Figure 3. For $0 < \zeta < 1$, the function $\Im(\gamma)$ has one positive zero in the range $(0, 1)$. Note that $\zeta < 1$ is the condition that resolution is to be increased in the region of the boundaries - the parameter range $\zeta \geq 1$ is not relevant. If the boundary layer is so thick that $\zeta \geq 1$, the program sets the grid to be linear (unstretched), ie

$$\Gamma = x + \tfrac{1}{2}(b+a). \tag{3.10}$$

The solution to (3.9) may be found quickly by numerical iteration. Hence Γ_0 is determined via (3.7), α_Γ may be evaluated from (3.6), and the function $\xi(x)$ is determined. The function $\eta(y)$ may then be evaluated in the same way.

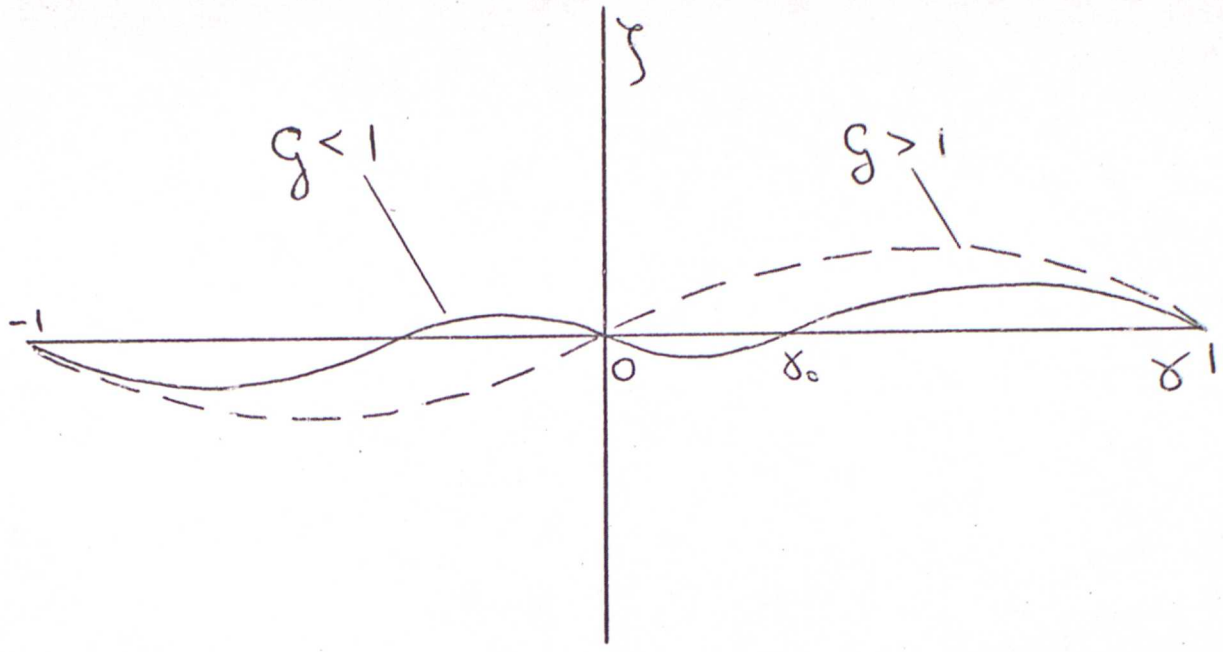

Figure 3

The function $\zeta(\gamma)$. For $\zeta<1$, $\zeta(\gamma)$ has one zero in the range $0<\gamma<1$. No such solution exists when $\zeta>1$. ($\zeta=1$ has an inflexion point at the origin).

Having evaluated the mapping functions, the grid points are defined as follows. The two sets each of radial and vertical grid points (see Figure 1) are defined, in (x, y) space, to be

$$x_i = (b-a)\left(\frac{2i-I}{2I-4}\right), \tag{3.11}$$

$$y_k = d\left(\frac{2k-K}{2K-4}\right), \tag{3.12}$$

for i in the range $(1, I)$, and k in $(1, K)$. The intermediate points are

$$\tilde{x}_i = \frac{1}{2}(x_i + x_{i-1}) \tag{3.13}$$

for $2 \leq i \leq I$; $\tilde{x}_1$ is defined such that

$$x_1 = \frac{1}{2}(\tilde{x}_1 + \tilde{x}_2). \tag{3.14}$$

Similarly,

$$\tilde{y}_k = \frac{1}{2}(y_k + y_{k-1}) \tag{3.15}$$

for $2 \le k \le K$, and

$$\tilde{y}_1 = 2y_1 - y_2 \,. \tag{3.16}$$

The (r, z) co-ordinates may now be determined from equations (3.1), with

$$r_i = \xi(x_i) \;;\quad \tilde{r}_i = \xi(\tilde{x}_i) \;;$$
$$z_k = \eta(y_k) \;;\quad \tilde{z}_k = \eta(\tilde{y}_k) \,. \tag{3.17}$$

For the purposes of finite differencing, we defined the grid increments

$$\delta r_i = r_i - r_{i-1} \;;\quad \tilde{\delta r}_i = \tilde{r}_i - \tilde{r}_{i-1} \,, \tag{3.18}$$

in the range $2 \le i \le I$ (they are not required at $i = 1$), and

$$\delta z_k = z_k - z_{k-1} \;,\quad \tilde{\delta z}_k = \tilde{z}_k - \tilde{z}_{k-1} \tag{3.19}$$

in $2 \le k \le K$.

3.2 Theory of finite differences on a non-uniform grid

The method used to represent derivatives on a stretched mesh is due to

Kalnay de Rivas (1972); the theory behind this method is outlined here.

Since $\tilde{x}_i$ lies midway between x_i and x_{i-1}, we have

$$\delta r_i = r_i - r_{i-1} = \xi(x_i) - \xi(x_{i-1})$$
$$= \Delta x . \xi'(\tilde{x}_i) + \frac{\Delta x^3}{24} \xi'''(\tilde{x}_i) + O(\Delta x^5) \qquad (3.20)$$

Now, the first derivative of any function ψ at, say, $r = \tilde{r}_i$ is given by

$$\left(\frac{\partial \psi}{\partial r}\right)_{r=\tilde{r}_i} = \left(\frac{\partial \psi}{\partial x}\right)_{x=\tilde{x}_i} \Big/ \left(\frac{d\xi}{dx}\right)_{x=\tilde{x}_i} . \qquad (3.21)$$

On the regular grid,

$$\left(\frac{\partial \psi}{\partial x}\right)_{x=\tilde{x}_i} = \frac{\psi(x_i) - \psi(x_{i-1})}{\Delta x} + O(\Delta x^2) \qquad (3.22)$$

so that

$$\left(\frac{\partial \psi}{\partial r}\right)_{r=\tilde{r}_i} = \frac{\psi(r_i) - \psi(r_{i-1})}{\Delta x . \xi'(\tilde{x}_i)} + O(\Delta x^2) . \qquad (3.23)$$

Now, provided that $\xi(x)$ is a smooth function in the sense that $\xi'''(x) \sim O(1)$, then from (3.20) and (3.23), we see that the expression

$$\left(\frac{\partial \psi}{\partial r}\right)_{r=\tilde{r}_i} \simeq \frac{\psi(r_i) - \psi(r_{i-1})}{\delta r_i} \equiv (\delta_r \psi)_{r=\tilde{r}_i} \qquad (3.24)$$

is accurate to $O(\Delta x^2)$. The requirement that $\xi(x)$ be smooth is equivalent to demanding that $\delta r_i - \delta r_{i-1}$ is not greater than $O(\Delta x^2)$, ie the stretching must not be too severe. In the same way as above, gradients at other grid points are found to be

$$\left(\frac{\partial \psi}{\partial r}\right)_{r=r_i} \simeq \frac{\psi(\tilde{r}_{i+1}) - \psi(\tilde{r}_i)}{\delta \tilde{r}_{i+1}} \equiv \left(\delta_r \psi\right)_{r=r_i},$$

$$\left(\frac{\partial \psi}{\partial z}\right)_{z=\tilde{z}_k} \simeq \frac{\psi(z_k) - \psi(z_{k-1})}{\delta z_k} \equiv \left(\delta_z \psi\right)_{z=\tilde{z}_k}, \qquad (3.25)$$

and $$\left(\frac{\partial \psi}{\partial z}\right)_{z=z_k} \simeq \frac{\psi(\tilde{z}_{k+1}) - \psi(\tilde{z}_k)}{\delta \tilde{z}_{k+1}} \equiv \left(\delta_z \psi\right)_{z=z_k}.$$

The second derivative is taken by evaluating the first derivative of one of the first derivatives, eg

$$\left(\frac{\partial^2 \psi}{\partial r^2}\right)_{r=\tilde{r}_i} \simeq \left[\delta_r\left(\delta_r \psi\right)\right]_{r=\tilde{r}_i} = \frac{\left(\delta_r \psi\right)_{r=r_i} - \left(\delta_r \psi\right)_{r=r_{i-1}}}{\delta r_i}, \qquad (3.26)$$

etc. This is again accurate to $O(\Delta x^2)$, subject to the same restriction on the severity of the stretching.

Despite the use of the staggered grid, some averaging is inevitably required. This is represented by, eg,

$$\left(\overline{\psi}^r\right)_{r=\tilde{r}_i} = \frac{1}{2}\left\{\psi(r_i) + \psi(r_{i-1})\right\} \qquad (3.27)$$

and is accurate to $O(\Delta x^2)$.

4 THE FINITE DIFFERENCE EQUATIONS

4.1 Formulation of the nonlinear advection terms

Aliassing errors in the nonlinear advective terms in the equations of motion can produce a slow numerical instability in the solutions. Arakawa (1966) showed that, in a streamfunction-vorticity model, these errors are controlled by the expression of the finite-difference derivative in flux form: so that, in our system, the expression

$$\mathcal{A} = \mathcal{A}_r + \mathcal{A}_z = u\frac{\partial T}{\partial r} + w\frac{\partial T}{\partial z} \tag{4.1}$$

is transformed, using the continuity equation, to

$$\mathcal{A} = \frac{1}{r}\frac{\partial}{\partial r}(ruT) + \frac{\partial}{\partial z}(wT) . \tag{4.2}$$

Using the staggered grid of Figure 1 and the notation of § 2.2, the equivalent finite-difference form is

$$\mathcal{A}_z = \left[\frac{\partial}{\partial z}(wT)\right]_{\tilde{r}_i,\tilde{z}_k} = \left[\delta_z(w\overline{T}^z)\right]_{\tilde{r}_i,\tilde{z}_k} . \tag{4.3}$$

This scheme assures conservation of both linear and quadratic integrals of the motion, because use of the streamfunction as a variable ensures exact solution of the continuity equation at all times. In a primitive equation model, however, this is not so, and continuity is dependent on solution of a Poisson equation for pressure, which is subject to (albeit small) truncation or iteration errors. This divergence error can produce a slow nonlinear instability (Williams 1969).

Linear integrals are not affected by this error.

It was shown by Piacsek and Williams (1970) that this instability may be overcome by reformulating the finite-difference form of the advective terms in such a way that conservation of quadratic integrals is maintained independent of the divergence error. This scheme may be written, in our system, as

$$\mathcal{A}_z = \left[\frac{1}{2}\left\{w\frac{\partial T}{\partial z} + \frac{\partial}{\partial z}(wT)\right\}\right]_{\tilde{r}_i,\tilde{z}_k} = \left[\frac{1}{2}\left\{\delta_z(w\bar{T}^z) + \overline{w\delta_z T}^z\right\}\right]_{\tilde{r}_i,\tilde{z}_k}, \quad (4.4)$$

which simplifies to the expression

$$\mathcal{A}_z = \frac{1}{2\delta z_k}\left(W^m_{i,k}T^m_{i,k+1} - W^m_{i,k-1}T^m_{i,k-1}\right). \quad (4.5)$$

This form has the additional advantage that it is simpler (and hence quicker to evaluate) than the corresponding flux-form derivative (4.3). It does have the disadvantage that errors, proportional to the divergence error, are introduced into linear integrals.

In the following model, the Piacsek-Williams "absolutely conserving" scheme is used to represent the advection terms in the equations of motion, thus ensuring that the kinetic energy integral is free from divergence errors. Such an error is, however, inevitably introduced into the angular momentum integral. This does not affect the numerical stability of the scheme in the same way as do errors in quadratic terms (since if these latter terms are bounded, stability is ensured, subject to certain other constraints to eliminate linear instability and time-splitting), and, as we shall see, the error vanishes as the system proceeds towards a steady state.

The heat advection terms are treated differently. The physically relevant

integrals deriving from the heat transfer equation are those of total heat balance and potential energy; the former is linear in temperature, while the second contains both linear and quadratic terms, by virtue of the equation of state (2.7). In most applications of this model, the rate of variation of the expansion coefficient with temperature, ρ_2 , is small, and the linear term in the equation of state is the dominant one. This being the case, the heat advection terms are represented by the Arakawa flux-form derivatives, to ensure error-free linear integrals. This results in an error proportional to ρ_2 in the potential energy integral, but this is always small, and vanishes in a steady state.

4.2 Representation of the diffusion terms

In order to ensure linear stability of the numerical scheme, certain upper limits have to be imposed on the timestep, Δt . Errors in the representation of advection or wave propagation are controlled if Δt satisfies the Courant-Friedrichs-Lewy condition

$$\Delta t < \Delta t_{CFL} = \frac{1}{2} \cdot \min \left\{ \frac{\delta_r}{|c_r|}, \frac{\delta_z}{|c_z|} \right\} \qquad (4.6)$$

where c_r is the maximum horizontal propagation speed of waves in the system, or the horizontal flow speed, whichever is the greater. c_z is the equivalent in the vertical direction. With the usual representation of diffusion terms, in a centred-difference time-marching model, the equivalent criterion is

$$\Delta t < \Delta t_D = \frac{1}{2} \left\{ \frac{\min(\delta_r^2, \delta_z^2)}{\max(\nu, \kappa)} \right\}_{\min} , \qquad (4.7)$$

satisfaction of this condition ensures that aliassing errors associated with the diffusion process are controlled.

Because of the fine resolution required in the parameter range relevant to laboratory experiments, (4.7) is frequently the more restrictive criterion (ie $\Delta t_D < \Delta t_{CFL}$), despite the smallness of ν and κ. In consequence, it is of practical advantage to use the Du Fort-Frankel scheme to represent the diffusion terms, thereby eliminating criterion (4.7) entirely (see Roache, 1972). There remains a formal loss of accuracy unless $\Delta t \ll \Delta t_D$; but, in a steady state (or a state whose evolution time is very long compared to diffusive time scales), the consequent errors vanish (or are small). Hence, in a time-dependent integration, errors may be introduced during periods of rapid evolution, but use of this scheme will introduce no errors into a steady state solution.

In practical terms, the Du Fort-Frankel scheme is formed by writing, for example, the diffusion terms $\tilde{\Delta}^2(\kappa,T)$ in equation (2.5) in usual finite-difference form, and then replacing $T_{i,k}^m$, wherever it appears, by $\frac{1}{2}(T_{i,k}^{m+1} + T_{i,k}^{m-1})$.

4.3 Finite-difference form of the governing equations

Using the schemes described above, the governing equations (2.1)-(2.3) and (2.5) are transformed into finite-difference prediction equations for u,v,w and T. These equations may be written as follows:

$$\delta_t \bar{u}^t = -\mathcal{A}_1(u) - \delta_r \pi + [2\Omega v]^* + \left[\frac{v^2}{r}\right]^* + D_u^\dagger , \qquad (4.8)$$

$$\delta_t \bar{v}^t = -\frac{1}{r}\mathcal{A}_1(rv) - \frac{2\Omega}{r}(\overline{ru}^r) + D_v^\dagger \qquad (4.9)$$

$$\delta_t \bar{w}^t = -\mathcal{A}_1(w) - \delta_z \pi + [\sigma]^* + D_w^\dagger , \qquad (4.10)$$

and

$$\delta_t \overline{T}^t = -Q_2(T) + D_T^{\dagger} , \qquad (4.11)$$

the right hand sides of the equations being interpolated at the mesh points appropriate to the quantities on the left hand side. In equation (4.10), σ is the buoyancy term, defined by the relation

$$\sigma = -\frac{g\rho}{\rho_0} = -g\left\{\rho_1(T-T_0) + \rho_2(T-T_0)^2\right\}. \qquad (4.12)$$

The asterisk labelling some of the terms denotes non-standard averaging. The buoyancy, σ, being a function of temperature, is evaluated at the grid points $(\tilde{r}_i, \tilde{z}_k)$; it is represented in the vertical velocity equation by the expression

$$\left[\sigma\right]^{*\,m}_{i,k} = -g\left\{\rho_1\left(\overline{T}^{z\,m}_{i,k} - T_0\right) + \rho_2\left(T^m_{i,k} - T_0\right)\left(T^m_{i,k+1} - T_0\right)\right\} \qquad (4.13)$$

Similarly, the Coriolis and centrifugal terms in the meridional velocity equation (4.8) are written

$$\left[2\Omega v\right]^* = \frac{\Omega}{\tilde{\delta r}_{i+1}}\left(v^m_{i,k}\,\delta r_i + v^m_{i+1,k}\,\delta r_{i+1}\right), \qquad (4.14)$$

and

$$\left[\frac{v^2}{r}\right]^* = v^m_{i,k}\,v^m_{i+1,k}\,\frac{\left(\tilde{r}^{\,2}_{i+1} - \tilde{r}^{\,2}_i\right)}{\tilde{r}_i\,\tilde{r}_{i+1}\,\tilde{\delta r}_{i+1}} , \qquad (4.15)$$

respectively. It is a simple matter to demonstrate that the expressions (4.13), (4.14) and (4.15) involve errors of order $(\Delta x^2, \Delta y^2)$.

The advection terms $\mathcal{A}_1$ and $\mathcal{A}_2$ are respectively the quadratically and linearly conserving forms of § 4.1; they may be written

$$\mathcal{A}_2(f) = \frac{1}{r}\delta_r\left[(\widetilde{ru})\,\overline{f}^{r}\right] + \delta_z\left[\widetilde{w}\,\overline{f}^{z}\right], \tag{4.16}$$

and

$$\mathcal{A}_1(f) = \frac{1}{2}\left\{\mathcal{A}_2(f) + \frac{1}{r}\overline{\left[(\widetilde{ru})\,\delta_r f\right]}^{r} + \overline{\left[\widetilde{w}\,\delta_z f\right]}^{z}\right\}, \tag{4.17}$$

where the tilde indicates that the quantities ru and w may need to be interpolated onto the appropriate mesh points.

The diffusion terms are:

$$\mathcal{D}_u = \frac{1}{r^2}\delta_r\left\{\nu r^3 \delta_r\left(\frac{u}{r}\right)\right\} + \delta_z\left\{\overline{\overline{\nu}}^{rz}\delta_z u\right\} + \frac{1}{r}\delta_r(\overline{ru})^{r}\delta_r\nu + \delta_r\overline{w}^{z}\delta_z\overline{\nu}^{r},$$

$$\mathcal{D}_v = \frac{1}{r^2}\delta_r\left\{\overline{\nu}^{r} r^3 \delta_r\left(\frac{v}{r}\right)\right\} + \delta_z\left\{\overline{\nu}^{z}\delta_z v\right\}, \tag{4.18}$$

$$\mathcal{D}_w = \frac{1}{r}\delta_r\left\{\overline{\overline{\nu}}^{rz} r\,\delta_r w\right\} + \delta_z\left\{\nu\,\delta_z w\right\} + \delta_z\overline{u}^{r}\delta_r\overline{\nu}^{z} + \delta_z\overline{w}^{z}\delta_z\nu,$$

and

$$\mathcal{D}_T = \frac{1}{r}\delta_r\left\{\overline{\kappa}^{r} r\,\delta_r T\right\} + \delta_z\left\{\overline{\kappa}^{z}\,\delta_z T\right\}.$$

Note that ν and κ are functions of temperature,

$$\nu = \nu_0\left\{1 + \nu_1(T-T_0) + \nu_2(T-T_0)^2\right\},$$

$$\kappa = \kappa_0\left\{1 + \kappa_1(T-T_0) + \kappa_2(T-T_0)^2\right\}, \tag{4.19}$$

and so are evaluated at the points $(\tilde{r}_i, \tilde{z}_k)$; hence the need for interpolating these quantities in equations (4.14). The superscript $(\dagger)$ in equations (4.8)-(4.11) signifies that, in these prediction equations, expressions (4.14) are to be modified to incorporate the Du-Fort-Frankel scheme, in the manner described in § 4.2.

Finally, the continuity equation (2.4) has the finite difference form

$$\Delta \equiv \frac{1}{r}\delta_r(ru) + \delta_z w = 0 . \tag{4.20}$$

4.4 Integrals of the finite-difference equations

(a) Angular Momentum

The finite-difference angular momentum integral is $2\pi\rho_0 A$, where

$$A^m = \sum_{i=2}^{I-1}\sum_{k=2}^{K-1} \tilde{r}_i^2 \, v_{i,k}^m \, \delta r_i \, \delta z_k . \tag{4.21}$$

Equation (4.9) integrates to give

$$\delta_t \bar{A}^t = \mathcal{J}_A^{(D)} + \mathcal{J}_A^{(V)} + \mathcal{J}_A^{(R)} + \delta_A + \delta_B , \tag{4.22}$$

where the terms on the right hand side are defined as follows. The dynamical flux of angular momentum through the boundaries is

$$\mathcal{J}_A^{(D)m} = \sum_{i=2}^{I-1} \tilde{r}_i^2 \left\{ w_{i,1}^m \, \bar{v}_{i,\frac{3}{2}}^{z\,m} - w_{i,K-1}^m \, \bar{v}_{i,K-\frac{1}{2}}^{z\,m} \right\} \delta r_i \; \ldots\ldots$$

$$\ldots + \sum_{k=2}^{K-1} \left\{ r_i u_{i,k}^m \, \overline{(\tilde{r}v)}^{r}_{\frac{3}{2},k}{}^{m} - r_{I-1} u_{I-1,k}^m \, \overline{(\tilde{r}v)}^{r}_{I-\frac{1}{2},k}{}^{m} \right\} \delta z_k , \tag{4.23}$$

and the viscous contribution is

$$\mathcal{F}_A^{(v)\,m} = \sum_{i=2}^{I-1} \tilde{r}_i^{\,2} \left\{ \bar{\nu}^{z\,m}_{i,K-\frac{1}{2}} \left(\delta_z v\right)^m_{i,K-\frac{1}{2}} - \bar{\nu}^{z\,m}_{i,\frac{3}{2}} \left(\delta_z v\right)^m_{i,\frac{3}{2}} \right\} \delta r_i \cdots$$

$$\cdots + \sum_{k=2}^{K-1} \left\{ \bar{\nu}^{r\,m}_{I-\frac{1}{2},k}\, r_{I-1}^3 \left[\delta_r\left(\frac{v}{r}\right)\right]^m_{I-\frac{1}{2},k} - \bar{\nu}^{r\,m}_{\frac{3}{2},k}\, r_1^3 \left[\delta_r\left(\frac{v}{r}\right)\right]^m_{\frac{3}{2},k} \right\} \delta z_k \,. \tag{4.24}$$

The third term is the mass flux term,

$$\mathcal{F}_A^{(R)\,m} = -2\Omega \sum_{i=2}^{I-1} \tilde{r}_i \mathcal{M}_i^m \delta r_i \,, \tag{4.25}$$

where the meridional mass flux is

$$\mathcal{M}_i^m = \sum_{k=2}^{K-1} \overline{(ru)}^{r\,m}_{i-\frac{1}{2},k} \cdot \delta z_k \,. \tag{4.26}$$

The last two terms on the right hand side of equation (4.22) are error terms, the first of which is the contribution from the Du Fort-Frankel scheme:

$$\delta_A^m = -2\cdot\Delta t^2 \sum_{i=2}^{I-1}\sum_{k=2}^{K-1} \tilde{r}_i^{\,2} \left[\delta_t(\delta_t v)\right]^m_{i,k} \left\{ \frac{\delta z_k}{r_i^3} \left[\frac{\overline{\nu^r r^3}}{\delta r}\right]^{r\,m}_{i-\frac{1}{2},k} + \delta r_i \left[\frac{\overline{\nu}^z}{\delta z}\right]^m_{i,k-\frac{1}{2}} \right\} . \tag{4.27}$$

The error involved is formally of order $\nu \frac{\Delta t^2}{\tau} \left(\frac{1}{\Delta r^2}, \frac{1}{\Delta z^2}\right)$, where τ is the

timescale of the motion; it is small provided that the evolution is slow enough, and vanishes in a steady state. The second error term is the contribution due to divergence error,

$$\delta_B^m = \frac{1}{2} \sum_{k=2}^{K-1} \sum_{i=2}^{I-1} \tilde{r}_i^2 V_{i,k}^m \Delta_{i,k}^m \delta r_i \delta z_k \,. \tag{4.28}$$

The error thus incurred in (4.21) is of order Δ ; as the divergence error Δ, is small, δ_B is also. Because the Poisson solver (5.1) is started with Π^{m-1} as the initial guess at the solution Π^m, the iterative scheme converges more accurately to the correct solution as a steady state is approached, and the divergence error (and hence also δ_B) vanishes.

(b) Heat balance.

The total heat content of the fluid is expressed by $2\pi c \rho_0 Q$, where

$$Q = \sum_{i=2}^{I-1} \sum_{k=2}^{K-1} \tilde{r}_i T_{i,k}^m \delta r_i \delta z_k \,, \tag{4.29}$$

and its evolution is described by the integral of equation (4.11), namely

$$\delta_t \overline{Q}^t = \overline{J}_Q^{(D)} + \overline{J}_Q^{(V)} + \delta_Q \,, \tag{4.30}$$

where the dynamic heat flux through the boundaries is

$$-\overline{J}_Q^{(D)m} = -\sum_{i=2}^{I-1} \left\{ W_{i,K-1}^m \overline{T}_{i,K-\frac{1}{2}}^{z\,m} - W_{i,1}^m \overline{T}_{i,\frac{3}{2}}^{z\,m} \right\} \tilde{r}_i \delta r_i \cdots$$

$$\cdots - \sum_{k=2}^{K-1} \left\{ r_{I-1} U_{I-1,k}^m \overline{T}_{I-\frac{1}{2},k}^{r\,m} - r_1 U_{1,k}^m \overline{T}_{\frac{3}{2},k}^{r\,m} \right\} \delta z_k \,, \tag{4.31}$$

and the conductive flux from the walls

$$\mathcal{J}_Q^{(v)\,m} = \sum_{i=2}^{I-1} \left\{ \bar{K}^{z}_{i,K-\frac{1}{2}}{}^{m} \left(\delta_z T\right)^{m}_{i,K-\frac{1}{2}} - \bar{K}^{z}_{i,\frac{3}{2}}{}^{m} \left(\delta_z T\right)^{m}_{i,\frac{3}{2}} \right\} \tilde{r}_i \, \delta r_i + \ldots$$

$$\ldots + \sum_{k=2}^{K-1} \left\{ \bar{K}^{r}_{I-\frac{1}{2},k}{}^{m} \, r_{I-1} \left(\delta_r T\right)^{m}_{I-\frac{1}{2},k} - \bar{K}^{r}_{\frac{3}{2},k}{}^{m} \, r_1 \left(\delta_r T\right)^{m}_{\frac{3}{2},k} \right\} \delta z_k \,. \qquad (4.32)$$

The final term is the Du Fort-Frankel error

$$\delta_Q^{m} = -\Delta t^2 \sum_{i=2}^{I-1} \sum_{k=2}^{K-1} \left[\delta_t(\delta_t T)\right]^{m}_{i,k} \left\{ \delta z_k \left(\frac{\overline{r \bar{K}^{r}}^{z}}{\delta r} \right)^{m}_{i-\frac{1}{2},k} + \tilde{r}_i \, \delta r_i \left(\frac{\overline{\bar{K}^{z}}^{r}}{\delta z} \right)^{m}_{i,k-\frac{1}{2}} \right\} ; \qquad (4.33)$$

this expression is similar to that in equation (4.26), and the comments on the errors involved apply here also.

(c) Kinetic energy

The total kinetic energy of the fluid is $2\pi\rho_0 \mathcal{E}_K$, and we define this quantity in the finite-difference scheme, at time $t = (m+\frac{1}{2})\Delta t$, to be

$$\mathcal{E}_K^{m+\frac{1}{2}} = \frac{1}{2} \sum\sum \left\{ u^m u^{m+1} + v^m v^{m+1} + w^m w^{m+1} \right\} (r \delta r)(\delta z) \,, \qquad (4.34)$$

where the summation is over all the fluid within the boundaries (so that some of the summation elements form less than a complete grid rectangle) and the increments $(r\,\delta r)$ and (δz) correspond to the rectangle appropriate to each velocity component. The evaluation of the rate of change of $\mathcal{E}_K$ is simplified

if we restrict attention to cases where any flow normal to the walls is constant, ie $\delta_t u = 0$ on the sidewalls, and $\delta_t w = 0$ on the endwalls. Then

$$
\begin{aligned}
(\delta_t \mathcal{E}_k)^m = & \sum_{i=2}^{I-2}\sum_{k=2}^{K-1} u_{i,k}^m \left(\delta_t \bar{u}^t\right)_{i,k}^m r_i \tilde{\delta r}_{i+1} \delta z_k \cdots \\
& + \sum_{i=2}^{I-1}\sum_{k=2}^{K-1} v_{i,k}^m \left(\delta_t \bar{v}^t\right)_{i,k}^m \tilde{r}_i \delta r_i \delta z_k \cdots \\
& + \sum_{i=2}^{I-1}\sum_{k=2}^{K-2} w_{i,k}^m \left(\delta_t \bar{w}^t\right)_{i,k}^m \tilde{r}_i \delta r_i \tilde{\delta z}_{k+1} \,.
\end{aligned}
\tag{4.35}
$$

One may then substitute for the components of acceleration, using the equations of motion (4.8)-(4.10), to find

$$
\delta_t \mathcal{E}_k = C_{pk} + \mathcal{F}_k^{(D)} - D_k + \delta_k^{(R)} + \delta_k^{(D)}
\tag{4.36}
$$

where the terms on the right hand side are defined as follows. The flux of kinetic and internal energy into the fluid is

$$
\begin{aligned}
\mathcal{F}_k^{(D)\,m} = & -\tfrac{1}{2}\sum_{i=2}^{I-2} \left\{ u_{i,K}^m \bar{w}^r_{i+\frac{1}{2},K-1}^m u_{i,K-1}^m - u_{i,2}^m \bar{w}^r_{i+\frac{1}{2},1}^m u_{i,1}^m \right\} r_i \tilde{\delta r}_{i+1} \cdots \\
& \cdots - \tfrac{1}{2}\sum_{i=2}^{I-1} \left\{ w_{i,K-1}^m \left(v_{i,K}^m v_{i,K-1}^m + 2\pi_{i,K-1}^m \right) - w_{i,1}^m \left(v_{i,2}^m v_{i,1}^m + 2\pi_{i,2}^m \right) \right\} \tilde{r}_i \delta r_i \cdots \\
& \cdots - \tfrac{1}{2}\sum_{i=2}^{I-1} \left\{ w_{i,K-1}^m \bar{w}^z_{i,K-\frac{3}{2}}^m w_{i,K-2}^m - w_{i,2}^m \bar{w}^z_{i,\frac{3}{2}}^m w_{i,1}^m \right\} \tilde{r}_i \delta r_i \cdots \\
& \cdots - \tfrac{1}{2}\sum_{k=2}^{K-1} \left\{ u_{I-1,k}^m \left(\bar{ru}^r\right)^m_{I-\frac{3}{2},k} u_{I-2,k}^m - u_{2,k}^m \left(\bar{ru}^r\right)^m_{\frac{3}{2},k} u_{1,k}^m \right\} \delta z_k \cdots \\
& \cdots - \tfrac{1}{2}\sum_{k=2}^{K-1} \left\{ (ru)_{I-1,k}^m \left[\left(\frac{v}{r}\right)_{I,k}^m (rv)_{I-1,k}^m + 2\pi_{I-1,k}^m \right] - (ru)_{1,k}^m \left[\left(\frac{v}{r}\right)_{2,k}^m (rv)_{1,k}^m + 2\pi_{1,k}^m \right] \right\} \\
& \cdots - \tfrac{1}{2}\sum_{k=2}^{K-2} \left\{ w_{I,k}^m \left(\bar{ru}^z\right)^m_{I-1,k+\frac{1}{2}} w_{I-1,k}^m - w_{2,k}^m \left(\bar{ru}^z\right)^m_{1,k+\frac{1}{2}} w_{1,k}^m \right\} \tilde{\delta z}_{k+1} \,,
\end{aligned}
\tag{4.37}
$$

while C_{PK} is the rate of conversion from potential to kinetic energy:

$$C_{PK}^{m} = \sum_{i=2}^{I-1}\sum_{k=2}^{K-1} W_{i,k}^{m} \left[\sigma\right]_{i,k}^{*m} \tilde{r}_i \, \delta r_i \, \tilde{\delta z}_{k+1} \, . \tag{4.38}$$

D_K is the rate of dissipation of kinetic energy; using the definition of the diffusion terms in equations (4.8)-(4.11), it is

$$\begin{aligned} D_K^{m} = & -\sum_{i=2}^{I-2}\sum_{k=2}^{K-1} r_i U_{i,k}^{m} \left(D_u^{\dagger}\right)_{i,k}^{m} \tilde{\delta r}_{i+1} \, \delta z_k \cdots \\ & -\sum_{i=2}^{I-1}\sum_{k=2}^{K-1} \tilde{r}_i V_{i,k}^{m} \left(D_v^{\dagger}\right)_{i,k}^{m} \delta r_i \, \delta z_k \cdots \\ & -\sum_{i=2}^{I-1}\sum_{k=2}^{K-2} \tilde{r}_i W_{i,k}^{m} \left(D_w^{\dagger}\right)_{i,k}^{m} \delta r_i \, \tilde{\delta z}_{k+1} \, . \end{aligned} \tag{4.39}$$

Equation (4.36) contains two error terms; the first is an error arising from the Coriolis terms in the equations of motion

$$\delta_k^{(R)\,m} = \sum_{k=2}^{K-1} \Omega \left\{ -V_{I-1,k}^{m} \left(ru\right)_{I-1,k}^{m} \delta \bar{r}_{I-1} - V_{2,k}^{m} \left(ru\right)_{1,k}^{m} \delta r_2 \right\} \delta z_k \, . \tag{4.40}$$

This term is zero if there is no source of fluid through the sidewalls; even if such a source exists, the error is small. With rigid no-slip sidewalls, $\left(\bar{V}_{I-\frac{1}{2},k}^{m} = \bar{V}_{\frac{3}{2},k}^{m} = 0\right)$, the error is $O(\Delta\tau^2)$; otherwise it is $O(\Delta\tau)$. The second error is proportional to the divergence error, and arises from the pressure - work term. It is

$$\delta_k^{(D)\,m} = \sum_{i=2}^{I-1}\sum_{k=2}^{K-1} \tilde{r}_i\, \pi_{i,k}^{m}\, \Delta_{i,k}^{m}\, \delta r_i\, \delta z_k \,. \tag{4.41}$$

The presence of this term in the energy integral does not promote instability, and the term vanishes as $\Delta \to 0$ in a steady state.

(d) Potential energy

We define the potential energy of the system to be $2\pi\rho_0 \mathcal{E}_p$, where

$$\mathcal{E}_p^{\,m} = -\sum_{i=2}^{I-1}\sum_{k=2}^{K-1} \sigma_{i,k}^{m}\, \tilde{z}_k\, \tilde{r}_i\, \delta r_i\, \delta z_k \,, \tag{4.42}$$

so that

$$\delta_t \bar{\mathcal{E}}_p^{\,t} = -\sum_{i=2}^{I-1}\sum_{k=2}^{K-1} (\delta_t \bar{\sigma}^t)_{i,k}^{m}\, \tilde{z}_k\, \tilde{r}_i\, \delta r_i\, \delta z_k \,. \tag{4.43}$$

From equations (2.7) and (4.12), we have

$$\delta_t \bar{\sigma}^t = -g\{\rho_1 + 2\rho_2(\bar{\bar{T}}^{tt} - T_0)\}\, \delta_t \bar{T}^t \,, \tag{4.44}$$

so that equation (4.11) may be used to find

$$\delta_t \bar{\sigma}^t = -g\{\rho_1 + 2\rho_2(\bar{\bar{T}}^{tt} - T_0)\}\{\mathcal{D}_T^t - Q_2(T)\} \tag{4.45}$$

whence we obtain an expression for the rate of change of potential energy,

$$\delta_t \bar{\bar{\xi}}_p^t = \mathcal{J}_p^{(D)} - C_{pK} - \mathcal{D}_p + \delta_p \,, \tag{4.46}$$

where C_{pK} is the energy conversion term (4.38). The flux of potential energy through the boundaries is

$$\mathcal{J}_p^{(D)\,m} = \sum_{i=2}^{I-1} \left\{ \tilde{z}_{K-1} W_{i,K-1}^m [\sigma]_{i,K-1}^{*\,m} - \tilde{z}_2 W_{i,1}^m [\sigma]_{i,1}^{*\,m} \right\} \tilde{r}_i \delta r_i \ldots .$$

$$\ldots . + \sum_{k=2}^{K-1} \left\{ r_{I-1} u_{I-1,k}^m [\bar{\bar{\sigma}}]_{I-\frac{1}{2},k}^{r\,*\,m} - r_1 u_{1,k}^m [\bar{\bar{\sigma}}]_{\frac{3}{2},k}^{r\,*\,m} \right\} \tilde{z}_k \delta z_k \,, \tag{4.47}$$

and the rate of dissipation of potential energy via thermal diffusion is expressed by the term

$$\mathcal{D}_p = g \sum_{i=2}^{I-1} \sum_{k=2}^{K-1} \left\{ \rho_1 + 2\rho_2 (\bar{\bar{T}}^{kt} - T_0)_{i,k}^m \right\} (\mathcal{D}_T^\dagger)_{i,k}^m \tilde{z}_k \tilde{r}_i \delta r_i \delta z_k \,. \tag{4.48}$$

The quadratic nature of the equation of state leads to an error term

$$\delta_p = -g\rho_2 \sum_{k=2}^{K-1} \sum_{i=2}^{I-1} \left\{ (T_{i,k}^m - T_0)^2 \Delta_{i,k}^m + 2\Delta t^2 [\delta_t(\delta_t T)]_{i,k}^m \right\} [\mathcal{Q}_2(T)]_{i,k}^m \tilde{\tilde{r}}_i \tilde{\tilde{z}}_k \delta r_i \delta z_k \tag{4.49}$$

This term is small, being of order $[\rho_2 . \max(\Delta, \Delta t^2)]$, and vanishes in a steady state; it does not promote numerical instability. This error could be

avoided by expressing the heat transfer equation (4.11) in terms of density (or buoyancy) rather than temperature.

(e) Asymptotic form of the integrals in a steady state with no source of fluid at the sidewalls.

If normal velocity components vanish on the sidewalls, then the dynamic flux terms in the integral relations above disappear (as do some of the error terms). Other error terms disappear towards a steady state, as $\delta_t \to 0$, and $\Delta \to \infty$ (see §5.2), and the expressions (4.22), (4.29), (4.36) and (4.46) take on the simple (and physically realistic) forms

$$\delta_t \bar{A}^t = \mathcal{J}_A^{(v)} ,$$

$$\delta_t \bar{Q}^t = \mathcal{J}_Q^{(v)} , \qquad (4.50)$$

$$\delta_t \mathcal{E}_k = C_{pk} - D_k ,$$

and $$\delta_t \bar{\mathcal{E}}_p^t = -C_{pk} - D_p ,$$

respectively.

4.5 The Poisson equation

The continuity equation is solved at every timestep by means of the solution of a Poisson equation for pressure. The meridional and vertical equations of motion, (4.8) and (4.10), may be written

$$\delta_t \bar{u}^t = -\delta_i \Pi + S_u - \tfrac{1}{2} \Delta t^2 \varepsilon_u \delta_t(\delta_t u) ,$$

and (4.51)

$$\delta_t \bar{w}^t = -\delta_z \Pi + S_w - \tfrac{1}{2} \Delta t^2 \varepsilon_w \delta_t(\delta_t w) ,$$

where S_u and S_w correspond to the right hand sides of the respective equations of motion without the pressure gradient terms and with $\mathcal{D}_u$ and $\mathcal{D}_w$ replacing the Du Fort-Frankel forms of the diffusion terms, and where

$$(\mathcal{E}_u)^m_{i,k} = \frac{1}{r_i^3 \tilde{\delta} r_{i+1}} \left\{ \frac{\nu^m_{i+1,k} \tilde{r}^3_{i+1}}{\delta r_{i+1}} + \frac{\nu^m_{i,k} \tilde{r}^3_i}{\delta r_i} \right\} + \frac{1}{\delta z_k} \left\{ \frac{\overline{\overline{\nu}}^{rz\,m}_{i+\frac{1}{2},k+\frac{1}{2}}}{\tilde{\delta} z_{k+1}} + \frac{\overline{\overline{\nu}}^{rz\,m}_{i+\frac{1}{2},k-\frac{1}{2}}}{\tilde{\delta} z_k} \right\} , \tag{4.52}$$

and

$$(\mathcal{E}_w)^m_{i,k} = \frac{1}{\tilde{r}_i \delta r_i} \left\{ \frac{\overline{\overline{\nu}}^{rz\,m}_{i+\frac{1}{2},k+\frac{1}{2}} r_i}{\tilde{\delta} r_{i+1}} + \frac{\overline{\overline{\nu}}^{rz\,m}_{i-\frac{1}{2},k+\frac{1}{2}} r_{i-1}}{\tilde{\delta} r_i} \right\} + \frac{1}{\tilde{\delta} z_k} \left\{ \frac{\nu^m_{i,k+1}}{\delta z_{k+1}} + \frac{\nu^m_{i,k}}{\delta z_k} \right\} .$$

Now, writing $\underset{\sim}{u} = (u,w)$, $\underset{\sim}{S} = (S_u, S_w)$, and defining the finite difference operators $\underset{\sim}{\nabla}.$ and ∇^2 such that

$$\underset{\sim}{\nabla}.(a,b) = \frac{1}{r} \delta_r (ra) + \delta_z b \tag{4.53}$$

and

$$\nabla^2 c = \frac{1}{r} \delta_r (r \delta_r c) + \delta_z (\delta_z c) , \tag{4.54}$$

equations (4.51) reduce to the divergence equation

$$\delta_t \overline{\Delta}^t \equiv \delta_t \left(\overline{\underset{\sim}{\nabla}.\underset{\sim}{u}}^t \right) = -\nabla^2 \overline{\Pi}^t + \underset{\sim}{\nabla}.\underset{\sim}{S} - \frac{\Delta t^2}{2} \underset{\sim}{\nabla}. \left\{ \mathcal{E}_u \delta_t(\delta_t u), \mathcal{E}_w \delta_t(\delta_t w) \right\} . \tag{4.55}$$

Neglect of the latter term involves an error of order $\left(\nu \frac{\Delta t}{\Delta x^2} \right) . \left(\frac{\Delta t}{\tau} \right)$, where τ is a typical timescale of the motion. Provided this quantity is not greater than $O(\Delta x^2)$, there is no formal loss of accuracy in the scheme as a whole, though the consequent divergence error contributes to the spurious terms

in the integrals of the system discussed in § 4.5. The term vanishes in a steady state. Neglecting this term, then, we satisfy continuity at time $t=(m+1)\Delta t$ by solving the equation

$$\Delta^{m+1} = -\nabla^2 \pi^m + \underline{\nabla}.\underline{S}^m + \frac{1}{2\Delta t}\left(\underline{\nabla}.\underline{u}\right)^{m-1} = 0 \,. \tag{4.56}$$

The inclusion of $\left(\underline{\nabla}.\underline{u}\right)^{m-1}$, the divergence error at $t=(m-1)\Delta t$, prevents a slow numerical instability which would otherwise arise (Williams 1969).

The boundary condition for π are found directly from the equations of motion (4.51), with the Du Fort-Frankel terms neglected (these are zero if there is no source of fluid at the boundaries). These conditions are:

$$\begin{aligned}
\left(\delta_r \pi\right)^m_{1,k} &= \left(S_u\right)^m_{1,k} - \left(\delta_t \bar{u}^t\right)^m_{1,k} \,, \\
\left(\delta_r \pi\right)^m_{I-1,k} &= \left(S_u\right)^m_{I-1,k} - \left(\delta_t \bar{u}^t\right)^m_{I-1,k} \,, \\
\left(\delta_z \pi\right)^m_{i,1} &= \left(S_w\right)^m_{i,1} - \left(\delta_t \bar{w}^t\right)^m_{i,1} \,,
\end{aligned} \tag{4.57}$$

and

$$\left(\delta_z \pi\right)^m_{i,K-1} = \left(S_w\right)^m_{i,K-1} - \left(\delta_t \bar{w}^t\right)^m_{i,K-1} \,.$$

Note that the velocity source functions S_u, S_w, cannot be evaluated directly on the boundaries, since they contain differentiated terms. However this is immaterial since the pressure at points outside the boundary is never needed when the velocity is stepped. At the boundaries therefore S_u and S_w may conveniently be made identically zero, and this zero-gradient boundary condition applied in the solution of the Poisson equation, which is discussed in § 5.1.

5 METHOD OF SOLUTION

5.1 ADI method for the Poisson equation

The Poisson equation (4.56) is solved by alternating direction iteration, optimised by the method of Wachspress (1966). The equation may be written

$$(O_r + O_z)\pi = F \tag{5.1}$$

where

$$F^m = \underline{\nabla}.\underline{S}^m + \frac{1}{2\Delta t}(\underline{\nabla}.\underline{u})^{m-1}, \tag{5.2}$$

and where the operators O_r and O_z are

$$[O_r\pi]^m_{i,k} = \frac{1}{\tilde{r}_i \delta r_i}\left\{\frac{r_i \pi^m_{i+1,k}}{\tilde{\delta r}_{i+1}} - \left(\frac{r_i}{\tilde{\delta r}_{i+1}} + \frac{r_{i-1}}{\tilde{\delta r}_i}\right)\pi^m_{i,k} + \frac{r_{i-1}\pi^m_{i-1,k}}{\tilde{\delta r}_i}\right\}, \tag{5.3}$$

and

$$[O_z\pi]^m_{i,k} = \frac{1}{\delta z_k}\left\{\frac{\pi^m_{i,k+1}}{\tilde{\delta z}_{k+1}} - \left(\frac{1}{\tilde{\delta z}_{k+1}} + \frac{1}{\tilde{\delta z}_k}\right)\pi^m_{i,k} + \frac{\pi^m_{i,k-1}}{\tilde{\delta z}_k}\right\}. \tag{5.4}$$

The method consists of introducing a set of iteration parameters τ_l, with l in the range $(1, L)$ and rewriting the Poisson equation (5.1) in the form

$$(\tau_l + O_r)\pi^{*l} = (\tau_l - O_z)\pi^{l-1} + F,$$

and (5.5)

$$(\tau_l + O_z)\pi^{l} = (\tau_l - O_r)\pi^{*l} + F,$$

where π^l is the result of the lth iteration towards the solution. The iteration is started by taking an interpolated initial field (see §5.2), and then equations (5.5) are solved in turn for $L=1,2\ldots.L$. The iteration parameters τ_L are chosen so that the convergence properties of the process are optimised. The method of Wachspress (1966) for $L=2^K$ is presented below.

If a single simultaneous eigenvector of both operators O_1 and O_2 is considered, it may be shown that the error after one iteration is

$$\frac{\tau-\lambda}{\tau+\lambda} \times \text{initial error} \qquad (5.6)$$

where λ is the eigenvalue. Clearly the optimum iteration parameter is $\tau=\lambda$. The range of eigenvalues supported by the grid is estimated as (α, β), where $\pi\alpha^{-1/2}$ is the longest side and $2\beta^{-1/2}$ is the shortest grid length. It is possible to find a curve (Fig 4), which is unique for a given number of iteration parameters, such that the largest error for any possible eigenvalue is minimised. (The behaviour outside the range (α,β) is immaterial.)

The iteration parameters are the zeros of this function; the error vanishes for the corresponding eigenvectors as indicated above. For other eigenvectors the residual error is

$$\left\{\prod_{L=1}^{L}\left(\frac{\tau_L-\lambda}{\tau_L+\lambda}\right)\right\}\times\text{initial error} \qquad (5.7)$$

For $L=1$, the solution is $\tau=\sqrt{\alpha\beta}$. For $L=2^K$, the problem may be

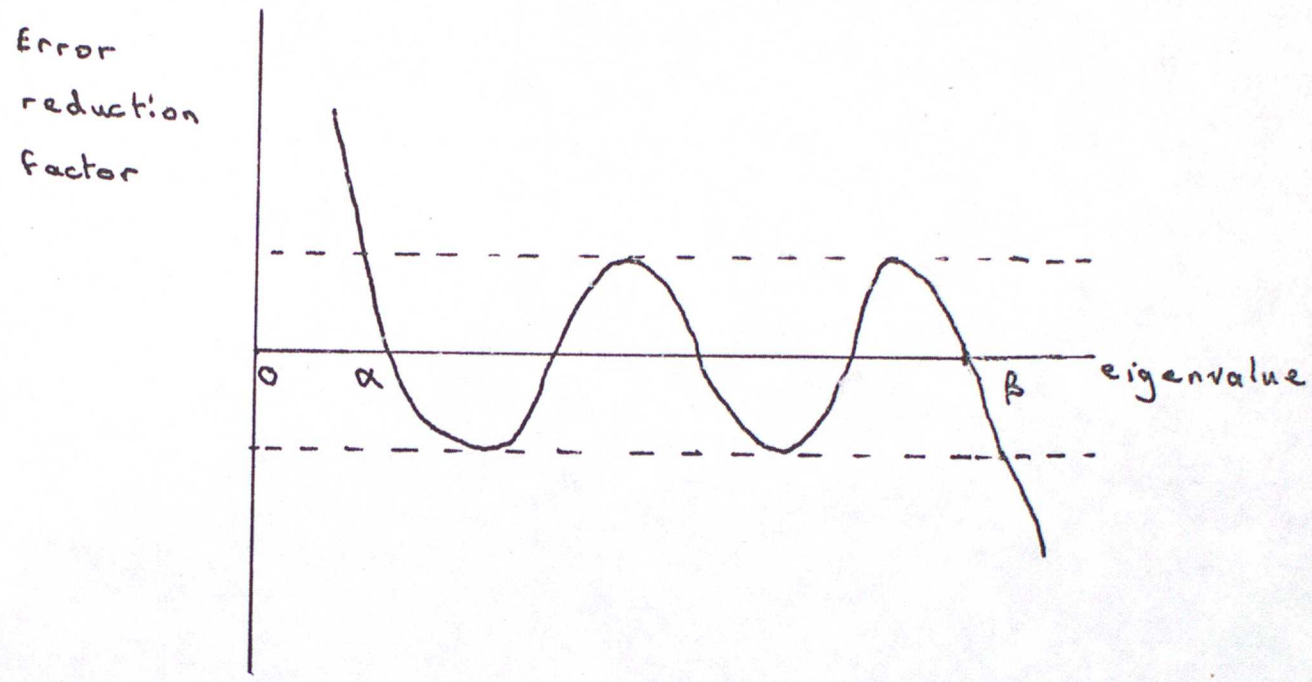

Figure 4 Error curve for eigenvalues of the ∇^2 operator

successively reduced to the problem of $L = 2^{K-1}$. The procedure is as follows. Take $\alpha_1 = \alpha$, $\beta_1 = \beta$, and then define

$$\alpha_{i+1} = \sqrt{\alpha_i \beta_i} \qquad (5.8)$$

and

$$\beta_{i+1} = \tfrac{1}{2}(\alpha_i + \beta_i) \qquad (5.9)$$

for $i = 2 \ldots K$, giving $\tau_{K+1} = \sqrt{\alpha_{K+1} \beta_{K+1}}$. The error for any given eigenfunction is reduced, at worst, by the factor

$$\frac{\beta_{K+1} - \tau_{K+1}}{\beta_{K+1} + \tau_{K+1}} = \frac{\tau_{K+1} - \alpha_{K+1}}{\tau_{K+1} + \alpha_{K+1}} \qquad (5.10)$$

Then each iteration parameter at one level yields two at the next level by solving the equation

$$\tau_i^2 - 2\tau_{i+1}\tau_i + \alpha_i \beta_i = 0 \qquad (5.11)$$

for $i = K \ldots 1$, so that eventually L iteration parameters are determined.

The first of equations (5.5) is now solved, row by row, by the method given below; the second equation is then solved column by column to complete the iteration cycle. Either of these two equations may be expressed in the form

$$A_j x_{j+1} + B_j x_j + C_j x_{j-1} = D_j \qquad (5.12)$$

where x is either π or π^* , and j represents either i or k (the other

index being fixed). The arrays A, B, C and D are defined for j in the range $(2, J-1)$ where $j=1$ and $j=J$ are the end points of the grid. The boundary conditions (4.57) take the form

$$x_2 - x_1 = 0 \ ,$$
$$x_J - x_{J-1} = 0 \ . \tag{5.13}$$

Equation (5.12) may be solved rapidly by the method of Richtmyer (1957); we write

$$x_j = b_j - a_j x_{j+1} \ . \tag{5.14}$$

Substitution into (5.12) gives the relations

$$a_j = \frac{A_j}{B_j - a_{j-1} C_j} \ , \tag{5.15}$$

and

$$b_j = \frac{D_j - b_{j-1} C_j}{B_j - a_{j-1} C_j} \ .$$

Comparing (5.14) with the first of the boundary conditions (5.13), we find

$$a_1 = 1 \ ; \quad b_1 = 0 \ . \tag{5.16}$$

Given these values, equations (5.15) may be used to find a_j, b_j for all j up to $J-1$. Then, using the second of the boundary conditions (5.13), we have

$$X_j = \frac{-b_{j-1}}{1 + a_{j-1}} \qquad (5.17)$$

Repeated use of equation (5.14) then constructs the solution $\underset{\sim}{X}$ for all j.

5.2 General outline of procedure

Given the fields u, v, w and T at time levels m and $(m-1)$, together with the pressure field π at times $(m-1)$ and $(m-2)$, the first step in the integration cycle is the evaluation of the pressure field π^m. The velocity source functions S_u^m and S_w^m are calculated, and then the pressure source function (the right hand side of equation (4.56)). The initial guess at the pressure field to begin the Poisson solver iteration, π°, is obtained by linear interpolation from the earlier fields:

$$(\pi^\circ)^m_{i,k} = 2\pi^{m-1}_{i,k} - \pi^{m-2}_{i,k} \qquad (5.18)$$

Thus, provided the previous fields are accurate enough, the iteration begins with a solution accurate to $O(\Delta t^2)$. In particular, as a steady state is approached, the accuracy of π° improves, so that the divergence error, Δ, $\to 0$. (It has already been noted that the error in the formulation of the pressure source function vanishes in a steady state.)

Having evaluated π^m, it is straightforward to use the prediction equations (4.8) - (4.11) to find u^{m+1}, v^{m+1}, w^{m+1} and T^{m+1} on all interior points. Application of the boundary conditions then provides the values of these fields on (or half a grid length outside) the boundaries. (These boundary conditions are applied by a subroutine separate from the main program, in order to allow the program to be used with any such conditions, subject to the restrictions mentioned in § 1). The fields π^{m-2}, u^{m-1}, v^{m-1}, w^{m-1} and T^{m-1} are discarded, and the integration cycle repeated for the next timestep.

In order to suppress the "time-splitting" instability that arises from the use of the "leap-frog" time-differencing scheme, the fields are smoothed in time at regular intervals. This is simply achieved by averaging over adjacent timesteps, and restarting the calculation with these values, and is usually performed every 21 timesteps.

The number of iterations required during the solution of the Poisson equation to yield a given accuracy is dependent on the structure of the pressure source function F in equation (5.1); as a matter of experience, it has been found that $\kappa = 3$ (ie 8 iterations) gives acceptable accuracy in most cases. After a "cold" start (ie from rest) however, κ is set equal to 5 for the first 80 timesteps, in order to obtain an accurate solution during the period of rapid evolution.

6 SUMMARY

A model has been described which is designed for the integration of the Navier-Stokes equations for the axisymmetric motion of a Boussinesq liquid contained in a rotating annulus. The finite difference scheme exhibits second order accuracy on a non-uniform mesh, and is formulated so as to generate the fewest possible errors in the physically important integrals of the motion. These errors vanish in a steady state for a system that has no sources or sinks of fluid at the boundaries; during the time-dependent stage of an integration, these errors are non-zero, but they are always small, and do not promote computational instability.

The model is based on a program developed by Drs S A Piacsek and A Warn-Varnas of the Naval Research Laboratories, Washington, DC; some amendments have been made in the present version, in order to provide improved accuracy and to allow greater generality.

REFERENCES

Arakawa, A. 1966 "Computational design for long term numerical integration of the equations of fluid motion. Two-dimensional incompressible flow, Pt 1", J. Comp. Phys., 1, 119-

Greenspan, H. P. 1968 The Theory of Rotating Fluids, Cambridge University Press.

Kalnay de Rivas, E. 1972 "On the use of nonuniform grids in finite-difference equations", J. Comp. Phys., 10, 202-210.

Pearson, C. E. 1965 "A computational method for viscous flow problems", J. Fluid Mech., 21, 611-622.

Piacsek, S. A. and Williams, G. P. 1970 "Conservation properties of convection difference schemes", J. Comp. Phys., 6, 392-405.

Richtmyer R. D. 1957 Difference Methods for Initial Value Problems. New York, Interscience 101-104.

Roache, P. J. 1972 Computational Fluid Dynamics. Hermosa Publ., Albuquerque, N.M.

Wachspress, E. L. 1966 Iterative Solution of Elliptic Systems. Prentice Hall, Englewood Cliffs, N.J.

Williams, G. P. 1967 "Thermal convection in a rotating fluid annulus: Part 1. The basic axisymmetric flow", J. Atmos. Sci., 24, 144-161.

Williams, G. P. 1969 "Numerical integration of the three-dimensional Navier-Stobes equations for incompressible flow", J. Fluid Mech., 37, 727-750.